Journal of ELECTRONIC MATERIALS, Vol. 45, No. 5, 2016
DOI: 10.1007/s11664-015-4291-6

Fabrication and Characterization of Large-Area Unpatterned and Patterned Plasmonic Gold Nanostructures

MINH THANH DO,[1,2,4] QUANG CONG TONG,[1,3] MAI HOANG LUONG,[1] ALEXANDER LIDIAK,[1] ISABELLE LEDOUX-RAK,[1] and NGOC DIEP LAI[1]

1.—Laboratoire de Photonique Quantique et Moléculaire, Ecole Normale Supérieure de Cachan, UMR 8537, CentraleSupélec, CNRS, Université Paris-Saclay, 94235 Cachan, France. 2.—Hanoi National University of Education, 136 Xuan Thuy, Cau Giay, Hanoi, Vietnam. 3.—Institute of Materials Science, Vietnam Academy of Science and Technology, 18 Hoang Quoc Viet, Cau Giay, Hanoi, Vietnam. 4.—e-mail: thanhdm@hnue.edu.vn

We report fabrication of Au nanoisland films on different substrates by thermally annealing a sputtered Au nanolayer and investigation of their structure, morphology, and optical properties. It was found that high-temperature annealing leads to transformation of the initial, continuous film into the forms of hillock and isolated island film. The final nanoisland films exhibit remarkably enhanced and localized plasmon resonance spectra with respect to the original sputtered film. The strong dependence of the resonance band spectra of the resulting structures on the annealing temperature and supporting substrate is presented and analyzed, suggesting that both of these factors could be used to tune the optical spectroscopic properties of such structures. Moreover, we propose and demonstrate a novel and effective approach for fabrication of patterned Au structures by thermally annealing the Au layer deposited onto modulated-surface substrates. The experimental results indicate that this method could become a promising approach for manufacturing plasmonic array structures, which have been extensively investigated and widely applied in many fields.

Key words: Gold structures, plasmonics, thermal annealing, laser interference lithography

INTRODUCTION

Discontinuous films or nanoisland structures of noble metals (e.g., Au, Ag, Cu) present optical properties that are notably different from those of bulk forms.[1,2] This special phenomenon is attributed to excitation of confined conduction-band electrons by external electromagnetic waves, namely localized surface plasmon resonance (LSPR), resulting in the appearance of a strong and localized extinction band (sum of scattering and absorption) and enhancement of the local electromagnetic field.[3] LSPR extinction band features including position and shape strongly depend on the structured morphology of the sample such as the size, shape, and interparticle distance, as well as the effective refractive index of the surrounding medium.[4] As a consequence, LSPR and its behavior pave the way to new developments in plasmonic-based optical devices and sensing applications.[4–8]

The optical properties of discontinuous films have been investigated and reported based on research into evaporation of metal layers.[2,9–11] An evaporated metal layer deposited in the form of nanoisland film shows the plasmon resonance effect, differing from the bulk-like response of thick metal layers. It is worth mentioning that the LSPR extinction band of evaporated films is too weak to be exploited for applications. Recently, thermal annealing was proposed as a simple technique for fabrication of metallic isolated-island structures, especially on Au material, using a thick evaporated metal layer.[12–14] However, previous research has

(Received October 10, 2015; accepted December 8, 2015; published online January 5, 2016)

not focused adequately on the influence of the fabrication conditions on the properties of the resulting metallic structures. Additionally, the conventional annealing method was known to be unable to fabricate patterned metallic arrays. To fabricate patterned metallic structures, a combination of several techniques with multiple processes should be used. For example, Ma et al.[15] suggested combining interference lithography with gold etching to fabricate large-area periodic structures. Song et al.[16] demonstrated another method by evaporating silver material on a monolayer opal template followed by a lift-off process. Siegel et al.[17,18] proposed to evaporate or sputter metallic materials onto an optically structured polymeric template. The combination of polymeric templates fabricated by laser interference lithography (LIL) with metallic deposition by either evaporation or sputtering seems very promising, because it enables realization of very large-area metallic structures.

In the present work, we first demonstrated fabrication of Au island films by thermally annealing sputtered Au layers and thoroughly investigated the influence of the annealing temperature and supporting substrate on the structure, morphology, and optical properties of the resulting Au films. Secondly, we propose a simple and effective route to fabricate patterned Au structures by annealing a metallic film previously sputtered onto a modulated-surface substrate. This fabrication procedure is simple, low cost, and promising for obtaining various plasmonic structured arrays, which could be applied in many fields.

FABRICATION AND CHARACTERIZATION OF GOLD ISLAND FILM STRUCTURES

Experimental Procedures and Characterization Techniques

Au layers of 20 ± 0.5 nm nominal thickness were directly deposited onto cleaned substrates using an Emitech K650 magnetron sputterer. The deposition conditions were direct-current Ar plasma, gas purity of 99.995%, and discharge current of 50 mA. The sputtering time was controlled to obtain the target thickness. To reveal the influence of the substrate on the formation of the Au island films during the annealing process, three different types of substrate were employed: microscope slide glass (Menzel-Glaser), microscope glass coated with indium tin oxide (ITO), and (c) microscope glass spin-coated with S1805 photoresist. Thermal annealing treatment was carried out in ambient condition at different temperatures between room temperature and 500°C (accuracy ±5°C) using a Nabertherm oven. Note that the highest annealing temperature was chosen to be lower than the glass-transition temperature of the glass substrate, $T_g \approx 557$°C. The annealing process involved three consecutive stages: an increasing temperature stage from room temperature to the desired target temperature at heating rate of 5°C min^{-1}, a constant annealing stage at the target temperature for 30 min, and a natural cooling down stage.

The structured morphology of the resulting structures was characterized by atomic force microscopy (AFM) and scanning electron microscopy (SEM). The optical properties of the structures were characterized by optical microscopy and ultraviolet–visible (UV–Vis) spectrometer.

Influence of Thermal Annealing Temperature

The surface morphology of the Au films on the glass substrate changed dramatically after the annealing process, as clearly shown by the AFM images in Fig. 1. It is evident that annealing leads to formation of discrete Au nanoislands from the continuous sputtered Au layer. The progression of this transformation can be observed by noting the dependence of the sample morphology on the annealing temperature. The sample annealed at 200°C exhibited hillock morphology containing holes, alternately incorporated with Au chains. Such hillock formation is probably caused by the unidentified thermal expansion of the glass substrate and the coated Au layer. In contrast, at 500°C, completely isolated nanoisland structure was obtained. It is well known that the melting point of Au nanoplatforms decreases rapidly with reduction of the particle size.[19,20] Therefore, it is assumed that, during the high-temperature annealing period, hillock-form Au layers melted and then coalesced into isolated particles.[14,21,22] Furthermore, as clearly observed from Fig. 1c, the Au islands display flat surfaces, indicating that the molten Au recrystallized during the high-annealing-temperature period.[23,24] Figure 2 shows microscopy images and UV–Vis spectra of Au samples obtained before and after annealing at different temperatures. The original sputtered film appears in dark blue, whereas all annealed samples exhibit reddish color, a trend that becomes increasingly apparent with higher calcination temperatures. The absorbance spectra of the annealed structures were qualitatively different in terms of both shape and height compared with the initial, sputtered film. A strong optical extinction band starts to appear for the sample heated at 200°C and becomes more obvious for the samples annealed at higher temperatures, whereas the original sputtered layer showed a broad optical band. The well-localized and remarkably enhanced extinction bands of the annealed samples are attributed to LSPR of gold nanoislands. However, we did not observe a clear shifting trend of the resonance peak wavelength of these samples with the optical extinction peaks being located at 560 nm, 575 nm, 578 nm, and 566 nm for annealing temperatures of 200°C, 300°C, 400°C, and 500°C, respectively. The same result was also previously observed and reported for Au island films obtained by annealing chemically synthesized colloidal Au nanoparticles.[25] This is due to the fact that the particle plasmon resonance depends

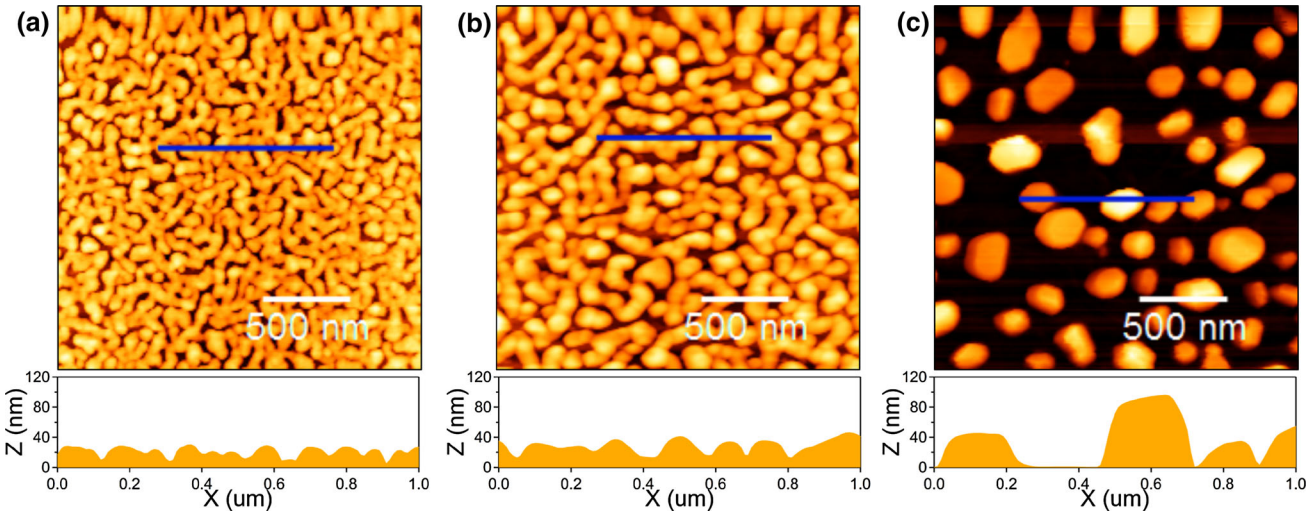

Fig. 1. AFM images of sputtered Au thin-film structures on glass substrate, obtained before annealing (a) and after annealing at 200°C (b) and 500°C (c).

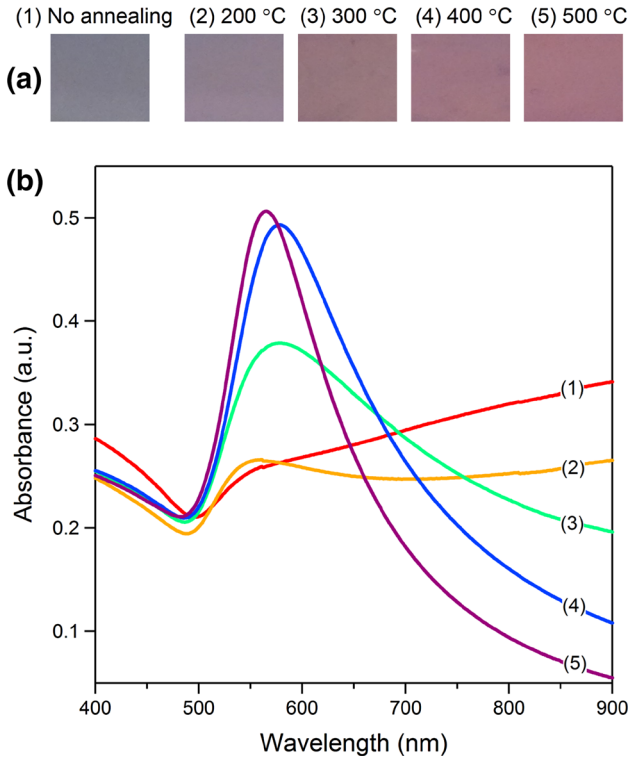

Fig. 2. Microscope images (a) and UV–Vis spectra (b) of sputtered Au thin films on glass substrate, obtained before and after annealing at different temperatures.

strongly on the size, shape, and aspect ratio (height/diameter) of the Au nanoislands, as well as on the medium surrounding them. As the annealing temperature increases, the structured morphology features of the islands, and consequently the total contact area of the sample with the environment, change in different ways, leading to nonmonotonic variation of the resonance spectrum. In addition, it can be seen that the extinction band of the samples annealed above 400°C did not change significantly with the temperature, as for the samples annealed at intermediate temperatures. This indicates that, in the temperature range below the glass-transition temperature of the glass substrate, 20-nm-thick sputtered gold film shows a high-quality plasmon resonance band after annealing at temperatures between 400°C and 500°C.

Influence of Substrate

Figure 3 shows SEM images of Au island film structures obtained after thermal annealing at 500°C of the metallic layer sputtered on different substrates. It is apparent that the substrate has a remarkably impact on the morphological features of the resulting island films. Au nanoislands with larger average diameter and smaller average height were produced on pure and ITO-coated glass as compared with the substrate coated with S1805. The results presented above show that the sputtered thin film melted and coalesced into isolated nanoislands during the annealing process. Therefore, the nature of the substrate, particularly its surface tension properties, is assumed to be a crucial factor directly impacting on the structured morphology and consequently the optical properties of the final Au island film. The surface tension of the substrate determines the interactions between the substrate and molten gold.[26] Additionally, the different thermal expansion of the substrate is also a vital factor affecting the features of the resulting metal structures. It should be noted that, during the thermal annealing, there are phase transformation processes of the S1805 photoresist, which has a glass-transition temperature of around 160°C and evaporates completely at temperatures above 350°C. Therefore, although the S1805 interlayers disappeared from the final Au

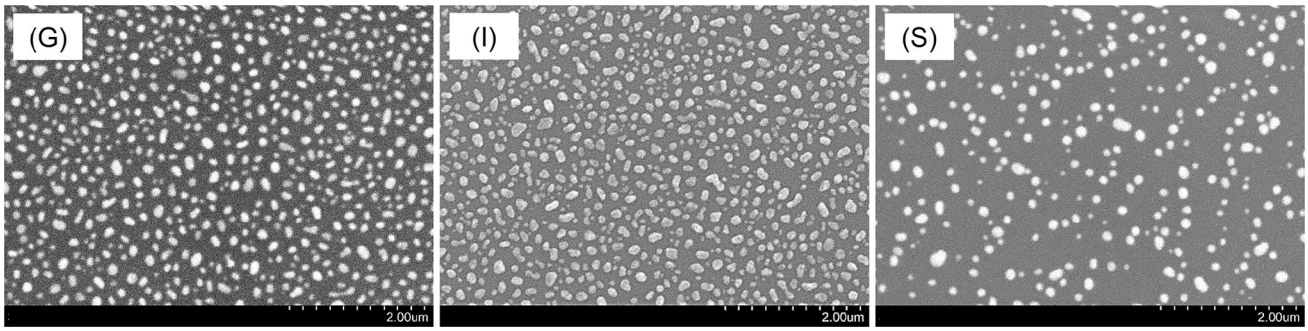

Fig. 3. SEM images of Au island film structures obtained by thermally annealing Au film sputtered on different substrates: glass (G), glass coated with ITO (I), and glass initially coated with S1805 photoresist (S). The annealing temperature was 500°C.

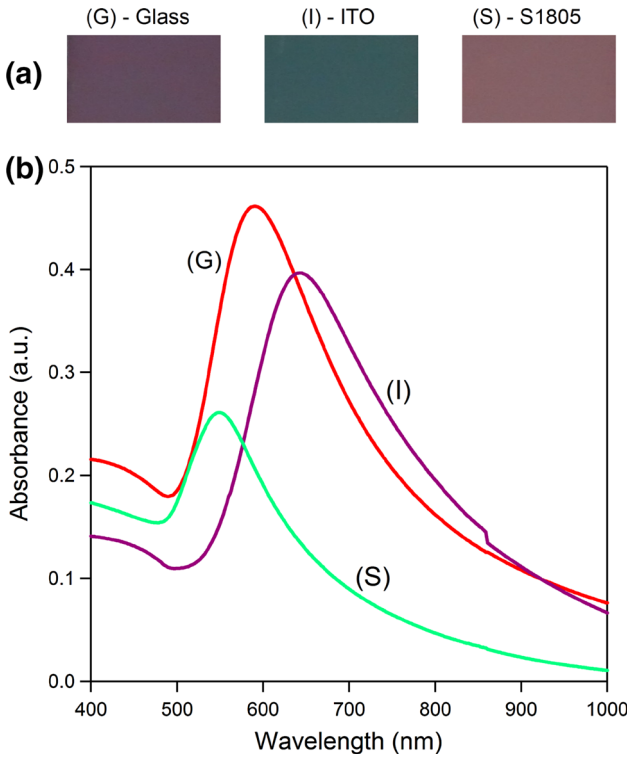

Fig. 4. Microscope images (a) and UV–Vis spectra (b) of Au island film structures obtained by annealing Au film sputtered on different substrates: glass (G), glass coated with ITO (I), and glass initially coated with S1805 photoresist (S). The annealing temperature was 500°C.

sample, they played a crucial role in the formation of Au islands during the annealing period. In contrast, the ITO nanolayer was not modified in the chosen range of annealing temperatures.

Figure 4 shows microscopy images and optical extinction spectra of Au island films on different substrates. The Au sample looks purple on pure glass, dark green on ITO, and light red on the initially photoresist-coated substrate. The corresponding UV–Vis spectra show that particle plasmons induce extinction centered at 643 nm on ITO, 590 nm on pure glass, and 550 nm on the initially S1805-coated glass substrate. Two dominant mechanisms account for the spectroscopic properties of the Au nanoislands on a substrate: (1) a structure-dependent effect, determined by the size, shape, and separation of the Au islands, and (2) the dependence on the environmental refractive index, with ITO having the largest (1.86) and pure glass the smallest value (1.51) among the substrates used, at wavelength of 633 nm. Therefore, the spectroscopic properties of the Au structures realized on different substrates are determined by manyfold related mechanisms that require further characterization. However, the supporting substrate has been shown to be an effective element that can be used to tune the optical response of such Au nanoisland films. Interestingly, use of an interlayer that can be completely eliminated during the annealing process is a promising practical approach to produce the desired metal structures. This concept is demonstrated in the next section.

FABRICATION OF STRUCTURED GOLD ARRAYS

Experimental Fabrication Process

Based on the above analysis, we propose a simple method for fabricating various structured Au arrays. The fabrication process, as shown schematically in Fig. 5a, involves two stages: (1) preparation of S1805 photoresist templates with the desired structures by laser interference lithography (LIL) and (2) sputtering of Au onto the templates and annealing of the whole system at high temperature. In particular, for this work, multiexposure two-beam LIL was used to produce the desired photoresist templates due to its simple setup and high-throughput fabrication, as described in our previous research.[27–29] The experimental setup of this technique is shown in Fig. 5b, in which the sample was fixed in a double-rotation holder. By adjusting the 2θ angle between the two incident laser beams and the rotation of the sample holder, we could easily manufacture S1805 templates with various structures and desirable lattice periods.[27] A series of S1805 templates with either line or pillar structure with modulation depth of 600 nm and period

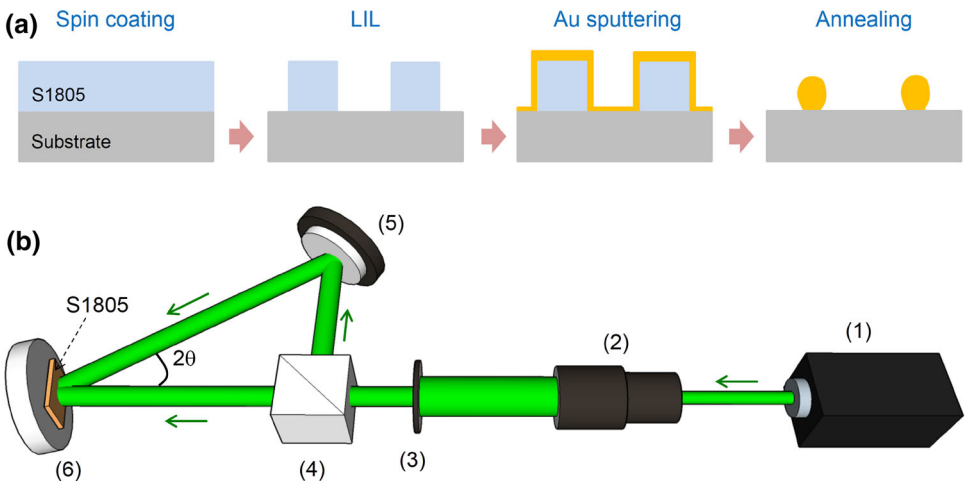

Fig. 5. (a) Schematic of fabrication process of structured Au arrays by combination of LIL and thermal annealing. (b) Schematics of multiexposure two-beam laser interference technique: (1) 532-nm laser source, (2) beam expander, (3) diaphragm, (4) beam splitter, (5) mirror, (6) double-rotation holder.

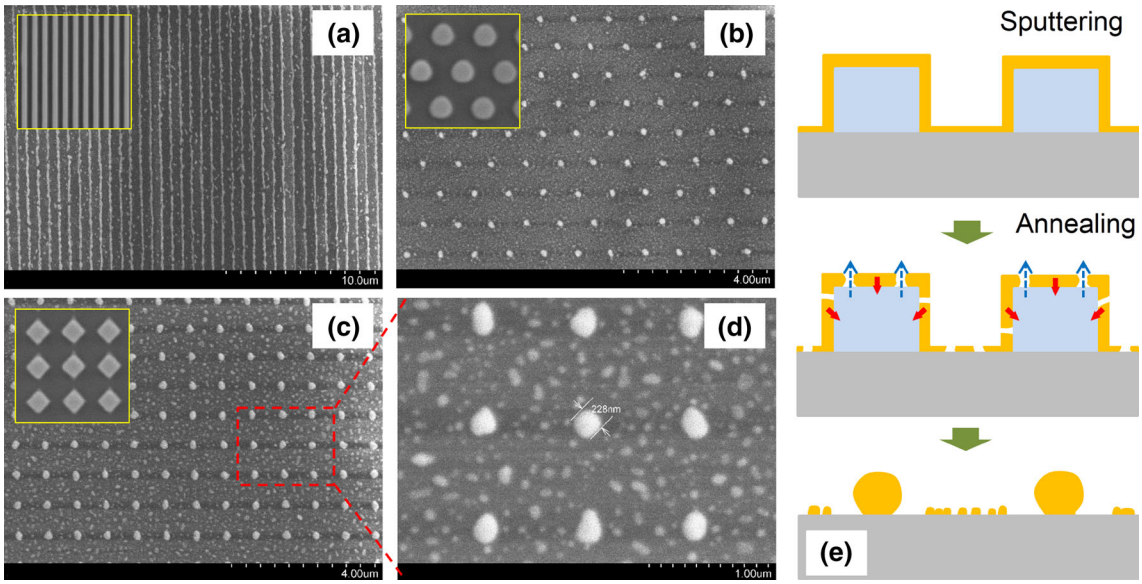

Fig. 6. SEM images of 1D and 2D Au structures fabricated by a combination of LIL and thermal annealing (a–d); schematic of mechanism explaining the formation of Au arrays (e). Insets in (a), (b), and (c) show SEM images (top view) of corresponding photoresist templates coated with a sputtered Au layer.

ranging from 0.5 μm to 1.0 μm were fabricated. Au layers were then deposited onto the photoresist structures. The deposition step for all samples was carried out with sputtering parameters allowing a 20-nm-thick layer to be formed on a flat substrate. The S1805-Au systems were subsequently annealed at 500°C for 30 min to evaporate the photoresist and obtain the final Au structures on the glass substrate.

EXPERIMENTAL RESULTS AND DISCUSSION

Figure 6a–d shows SEM images of various patterned Au structures fabricated using the proposed procedure as illustrated in Fig. 5a. The corresponding S1805 templates coated with a sputtered Au layer before annealing are presented in the inset to each image. It is evident that, after the annealing process, the photoresist was removed and the Au material remained on the substrate in the form of periodic arrays. The one-dimensional (1D) metal grating consisted of continuous and homogeneous nanowires, although a few break due to the annealing. In contrast, the two-dimensional (2D) Au structures showed high-quality arrays of Au nanodots. As can be seen for all samples, the lattice period of the resulting metal structure was similar to that of the corresponding original S1805 template obtained by the LIL process. Note that small Au nanoparticles with diameter of

around 50 nm remained randomly outside the dominant Au periodic arrays. The homogeneous area of the fabricated Au structures was 1.0 cm × 1.0 cm, similar to the size of the diaphragm used in the LIL process; this could be easily extended to larger sizes if desired. The mechanism explaining the formation of the structured Au arrays is illustrated in Fig. 6e. After the sputtering process, a thin layer of Au was isotropically deposited onto the top and side-walls of the S1805 lines for 1D and pillars for 2D structures, as well as the blank areas of the glass surface. During the annealing process, when the temperature was increased to above 200°C, the Au layer started to melt and broke down into segments, allowing the S1805 to evaporate gradually, as demonstrated by the dotted blue arrows. The loss of S1805 due to evaporation led to aggregation of the melting Au segments, following the direction of the bold red arrows. At high temperature of around 500°C, the S1805 evaporated completely and all the Au initially coated on the S1805 aggregated and coalesced into localized and well-arranged dots or lines. The final metal structures would therefore have a geometrical morphology and period similar to those of the photoresist template. As the size of the S1805 line or pillar decreased, the amount of Au coating also decreased, resulting in a smaller and thinner Au line or dot. Additionally, according to the results presented above, after annealing at high temperature, the thin Au layers deposited on the blank glass areas were transformed into random isolated nanoparticles that remained outside the dominant array structure. Patterned noble-metal structures have been researched and applied extensively in many fields. It has been reported both theoretically and experimentally that patterned plasmonic structures exhibit highly controllable and enhanced plasmonic behavior as compared with unpatterned ones.[30,31] This simple and effective method for fabrication of plasmonic structures is therefore worthy of research and exploitation. Our approach shows obvious advantages such as low cost, simplicity, and high-throughput fabrication in comparison with conventional methods such as ion-beam milling,[32,33] lithography with lift-off,[15,22] and solution processing.[34,35] Generally, by using the proposed technique, we are able to fabricate various Au structures in periodic, quasiperiodic, or arbitrary networks with controllable lattice parameters. The optical response of the final metal networks is contributed by their structured morphology, which depends on the photoresist template. The LIL process therefore plays a vital role in enabling the behavior as well as the applicability of the resulting metal structures, which is currently under investigation.

CONCLUSIONS

Various Au nanostructures were fabricated, and characterized by different techniques. We first fabricated Au island films on different substrates by a conventional thermal annealing process. Experimental characterization showed that the high-temperature annealing process melted the sputtered Au thin film, leading to formation of isolated Au nanoislands exhibiting enhanced plasmon resonance with respect to the original sputtered layer. The impact of fabrication conditions such as the annealing temperature and supporting substrate was investigated and is systematically presented. Both of these are effective factors that can be used to tune the optical behavior of the metal structures. Secondly, a novel method combining the thermal annealing process and the LIL technique is proposed for fabricating large-area patterned Au structures. The mechanism of formation of the Au structures has been analyzed; due to the thermal annealing process, the Au nanolayer on the top and side-wall of the S1805 is melted and broken down, allowing the S1805 to evaporate during this process. During the removal of the S1805 cores, the molten Au nanosegments simultaneously coalesced and formed into well-arranged structures. The geometry of the S1805 template determined the geometry of the resulting Au structure. Therefore, desired metallic 1D and 2D structures could be rapidly realized by a simple interference technique, paving the way to numerous plasmonic and photonic applications.

ACKNOWLEDGEMENTS

The authors acknowledge Mr. Arnaud Brosseau and Mr. Joseph Lautru for their support in AFM and SEM measurements, respectively.

REFERENCES

1. U. Kreibig and M. Vollmer, *Optical Properties of Metal Clusters* (Heidelberg: Springer, 1995), p. 50.
2. R.H. Doremus, *J. Appl. Phys.* 37, 2775 (1966).
3. P.K. Jain, K.S. Lee, I.H. El-Sayed, and M.A. El-Sayed, *J. Phys. Chem. B* 110, 7238 (2006).
4. E. Hutter and J.H. Fendler, *Adv. Mater.* 16, 1685 (2004).
5. T. Xu, Y.K. Wu, X. Luo, and L.J. Guo, *Nat. Commun.* 1, 1 (2010).
6. Y. Lin, T. Zhai, Q. Ma, H. Liu, and X. Zhang, *Opt. Express* 21, 11315 (2013).
7. A.G. Brolo, *Nat. Photon.* 6, 709 (2012).
8. V.G. Kravets, F. Schedin, R. Jalil, L. Britnell, R.V. Gorbachev, D. Ansell, B. Thackray, K.S. Novoselov, A.K. Geim, A.V. Kabashin, and A.N. Grigorenko, *Nat. Mater.* 12, 304 (2013).
9. S. Norrman, T. Andersson, C.G. Granqvist, and O. Hunderi, *Phys. Rev. B* 18, 674 (1978).
10. P. Lansaker, J. Backholm, G. Niklasson, and C. Granqvist, *Thin Solid Films* 518, 1225 (2009).
11. J. Siegel, O. Lyutakov, V. Rybka, Z. Kolska, and V. Švorčík, *Nanoscale Res. Lett.* 6, 96 (2011).
12. G. Gupta, D. Tanaka, Y. Ito, D. Shibata, M. Shimojo, K. Furuya, K. Mitsui, and K. Kajikawa, *Nanotechnology* 20, 025703 (2009).
13. A. Serrano, O. Rodrıguez de la Fuente, and M.A. Garcıa, *J. Appl. Phys.* 108, 074303 (2010).
14. V. Švorčík, O. Kvıtek, O. Lyutakov, J. Siegel, and Z. Kolska, *Appl. Phys. A* 102, 747 (2011).
15. F. Ma, M.H. Hong, and L.S. Tan, *Appl. Phys. A* 93, 907 (2008).
16. Y. Song and H.E. Elsayed-Ali, *Appl. Surf. Sci.* 256, 5961 (2010).
17. J. Siegel, J. Heitz, and V. Švorčík, *Surf. Coat. Technol.* 206, 517 (2011).
18. J. Tuma, O. Lyutakov, I. Huttel, J. Siegel, J. Heitz, Y. Kalachyova, and V. Švorčík, *J. Mater. Sci.* 48, 900 (2013).

19. P. Buffat, J. Borel, *Phys. Rev. A* 13(6) (1976).
20. P.R. Couchman and W.A. Jesser, *Nature* 269, 481 (1977).
21. T. Karakouz, A.B. Tesler, T.A. Bendikov, A. Vaskevich, and I. Rubinstein, *Adv. Mater.* 20, 3893 (2008).
22. M. Bechelany, X. Maeder, J. Riesterer, J. Hankache, D. Lerose, S. Christiansen, J. Michler, and L. Philippe, *Cryst. Growth Des.* 10, 587 (2010).
23. V.L. De Los Santos, D. Lee, J. Seo, F.L. Leon, D.A. Bustamante, S. Suzuki, Y. Majima, T. Mitrelias, A. Ionescu, and C.H. Barnes, *Surf. Sci.* 603(19), 2978 (2009).
24. V. Svorcık, O. Kvıtek, J. Rıha, Z. Kolska, and J. Siegel, *Vacuum* 86, 729 (2012).
25. H. Liu, X. Zhang, and Z. Gao, *Photon. Nanostruct. Fund. Appl.* 8, 131 (2010).
26. X. Zhang, H. Liu, and S. Feng, *Nanotechnology* 20, 425303 (2009).
27. N.D. Lai, W.P. Liang, J.H. Lin, C.C. Hsu, and C.H. Lin, *Opt. Express* 13, 9605 (2005).
28. N.D. Lai, J.H. Lin, Y.Y. Huang, and C.C. Hsu, *Opt. Express* 14, 10746 (2006).
29. N.D. Lai, C.C. Hsu, D.B. Do, J.H. Lin, T.S. Zheng, W.P. Liang, Y.Y. Huang, and Y. Di Huang, *Fabrication of Two and Three-Dimensional Photonic Crystals and Photonic Quasi Crystals by Interference Technique* (INTECH Open Access Publisher, 2011), p. 255.
30. Y. Chu, E. Schonbrun, T. Yang, and K.B. Crozier, *Appl. Phys. Lett.* 93, 181108 (2008).
31. A.D. Humphrey and W.L. Barnes, *Phys. Rev. B* 90(7) (2014).
32. T.W. Ebbesen, H.J. Lezec, H.F. Ghaemi, T. Thio, and P.A. Wolff, *Nature* 391, 667 (1998).
33. G. Si, X. Jiang, J. Lv, Q. Gu, and F. Wang, *Nanoscale Res. Lett.* 9, 1 (2014).
34. X. Zhang, B. Sun, R.H. Friend, H. Guo, D. Nau, and H. Giessen, *Nano Lett.* 6, 651 (2006).
35. X. Zhang, H. Liu, and Z. Pang, *Plasmonics* 6, 273 (2011).